In situ-loading transfection of short single- and double-stranded DNAs by supramolecular organic frameworks

Bo Yang[1], Xiao-Dan Zhang[2], Jian Li[3], Jia Tian[1], Yi-Peng Wu[1], Lu Zhou[2], Fa-Xing Yu[3], Ruibing Wang[4], Yi Liu[5], Hui Wang[1], Dan-Wei Zhang[1] & Zhan-Ting Li[1]

Abstract

Short DNAs represent an important class of biomacromolecules that are widely applied in gene therapy, editing and modulation. However, the development of simple and reliable methods for their intracellular delivery is still a challenge. We herein describe that seven water-soluble homogeneous supramolecular organic frameworks (SOFs) with well-defined pore size and high stability in water can realize in-situ inclusion of ss- and dsDNAs (21, 23 and 58 nt) and deliver them into two normal cells or six cancer cells. Fluorescence quenching experiments for single and double end-labeled ss-DNAs (21 and 58 nt) support that the DNA sequences can be completely included by the frameworks. Confocal laser scanning microscopy and flow cytometry reveal that five SOFs exhibit excellent transfection efficiency that outperform the commercial reagent Lipo2000 even at low SOF-nucleic acid ratios. In addition to higher transfection efficiency, the water-soluble self-assembled SOF carriers have the advantages of convenient preparation, high stability and in situ DNA inclusion, which are all crucially required for practical use.

[1]Department of Chemistry, Shanghai Key Laboratory of Molecular Catalysis and Innovative Materials and Collaborative Innovation Center of Chemistry for Energy Materials (iChEM), Fudan University, Shanghai 200438, China. [2]Department of Medicinal Chemistry, School of Pharmacy, Fudan University, 826 Zhangheng Road, Shanghai 201203, China. [3]Children's Hospital and Institutes of Biomedical Sciences, Fudan University, Shanghai 200032, China. [4]State Key Laboratory of Quality Research in Chinese Medicine, Institute of Chinese Medical Sciences, University of Macau, Taipa, Macao, China. [5]The Molecular Foundry, Lawrence Berkeley National Laboratory, Berkeley, California 94720, U.S.A. These authors contributed equally: Bo Yang, Xiao-

Na Zhang. Correspondence and requests for materials should be addressed to L.Z. (email: zhoulu@fudan.edu.cn) or Y.-X.Y. (fxyu@fudan.edu.cn) or to Y.L. (email: yliu@lbl.gov) or to Z.-T.L. (email: ztli@fudan.edu.cn).

Intracellular delivery of exogenous DNAs is a key factor for the development of gene therapy and editing[1-4]. Owing to their clinical applications and potentials, short DNAs have been important targets of delivery studies[5-8]. Viral vectors have been demonstrated to be highly efficient, but suffer from safety concern, high cost, and scale-up difficulty[9-11]. In the past two decades, non-viral cationic vectors, in particular liposomes[12,13], dendrimers[14-16], polymers[17-21], and nanoparticles[22-25], have been extensively investigated through multivalent electrostatic interaction with DNAs and achieved considerable success. However, relatively high cytotoxicity, limited transfection efficiency and lack of precision remain as obstacles for their clinical trials. Materials with defined porosity are structurally suitable for DNA inclusion because their inherent pores are expected to avoid unrequired entanglement of included DNAs, which may restrain reversible gene release. Nevertheless, reported vectors of this family have been limited to solid-state structures[26-28], the slow metabolism of which may cause detrimental internal aggregation. The development of water-soluble cationic porous frameworks that are able to operate in a homogeneous manner is expected to integrate the advantages of the above two kinds of vectors. However, this possibility has not been realized.

We have recently developed a general strategy for the generation of water-soluble three-dimensional (3D) supramolecular organic frameworks (SOFs) from the co-assembly of preorganized multicationic monomers with cucurbit[8]uril (CB[8])[29-32]. As a family of self-assembled water-soluble porous polyelectrolytes, diamondoid SOFs were demonstrated to adsorb anionic guests and deliver adsorbed chemotherapeutic reagents, such as pemetrexed, into tumor cells.[33] We herein describe that two kinds of SOFs, which have a pore size of approximately 2.2 or 2.0 nm, can include short single- or double-stranded (ss- and ds-) DNAs (21, 23 and 58 nt), which is readily realized by simply mixing the two samples, and deliver the DNAs into normal and cancer

cells. We demonstrate that, out of 126 delivery experiments, 98 cases can achieve a delivery efficacy surpassing that of Lipo2000, a commercial transfection reagent.

Results

Monomers of SOF vectors. Diamondoid SOFs are regular porous supramolecular polyelectrolytes co-assembled by tetracationic monomers and CB[8][31,32]. With (4-phenyl)pyridinium as binding subunit through the CB[8] encapsulation-enhanced dimerization binding motif[34-37], the water-soluble polycationic frameworks form ordered pores that have a size of approximately 2.2 nm[29]. Previously, we demonstrated their robustness as molecular drug carriers to attain intracellular transport and low cytotoxicity[33,40]. Given the polyanionic feature of DNA and the approximately 2.0 nm diameter of dsDNAs[38,39], it is conceivable that diamondoid SOFs are suitable carriers for the inclusion of both ss- and dsDNAs through multivalent electrostatic interactions,[41,42] which is the basis for all reported polycationic DNA carriers. The homogeneity of SOFs is expected to allow for quick DNA inclusion and reversible release after intracellular delivery. **SOF-a-g**, which are constructed from **1a-g** and CB[8] (1:2), are thus used for exploiting this potential (Figure 1). The first six frameworks have been reported for the inclusion of discrete organic guests and for SOF postmodification[29,43], while **SOF-g** was designed to test the generality of this new delivery strategy.

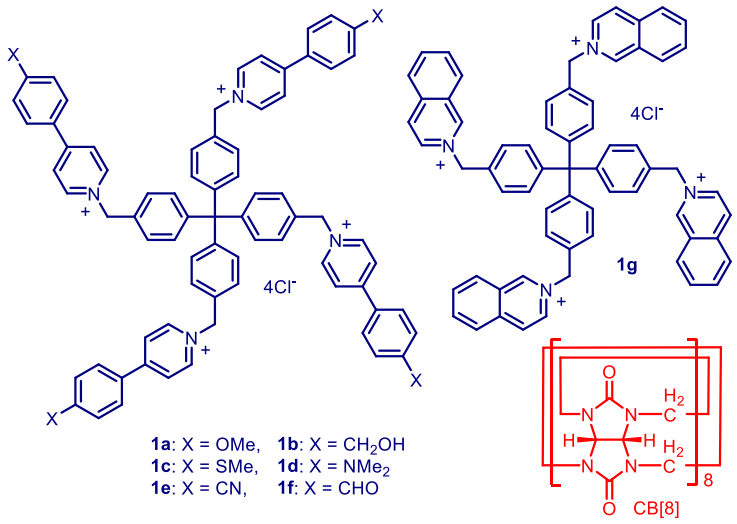

Fig. 1 | Compounds used in this study. The structures of compounds **1a–g** and CB[8].

Characterization and cytotoxicity of SOF-g. The synthesis and characterization of the new SOF-g was discussed here in detail as an example since SOF-a-f was prepared and characterized previously. Tetrahedral monomer **1g** was prepared from tetrakis(4-(bromomethyl)phenyl)methane and isoquinoline followed by ion exchange. **SOF-g** was prepared by dissolving the 1:2 mixture of **1g** and CB[8] in hot water. The X-ray crystallographic structure of the 2:1 mixture of *N*-benzylisoquinolinium bromide (**2**) with CB[8] revealed that two isoquinolinium moieties were entrapped in the cavity of the CB[8] (Supplementary Figure 1), which evidenced the 2:1 binding motif of **1g** and CB[8]. ^{1}H NMR titration experiments in D_2O for **2** and **1g** with CB[8] further supported this 2:1 binding motif in water (Supplementary Figure 2). Isothermal titration calorimetry afforded (apparent) binding constant of 4.8×10^{11} M^{-2} for [**2**]$_2$⊂CB[8] and 2.5×10^{12} M^{-2} for the 2:1 complex of the appended isoquinolinium subunits of **1g** and CB[8] (Supplementary Figure 3), suggesting high stability of this binding motif and positive cooperativity for the appended isoquinolinium subunits of **1g**.[29] 2D ^{1}H NMR diffusion-ordered spectroscopic experiments for the mixture of **2** (2:1) and **1g** (0.5:1) with CB[8] (1.0 mM) in D_2O gave rise to a diffusion coefficient (*D*) of 2.5×10^{-10} and 1.1×10^{-10} m^2 s^{-1} for the signals of both components (Supplementary Figure 4), indicating that **1g** and CB[8] formed larger supramolecular entities. Dynamic light scattering experiments for the 1:2 solutions of **1g** and CB[8] revealed the formation of large aggregates, with the hydrodynamic diameter (D_H) ranging from 91 nm (CB[8] = 2 mM) to 31 nm (CB[8] = 0.03 mM) (Supplementary Figure 5). Moreover, the D_H values underwent little changes after the solutions were left to stand for 48 hours. Solution-phase synchrotron small-angle X-ray-scattering (SAXS) profile of the 1:2 solution of **1g** and CB[8] (2.0 mM) exhibited a very weak and broad, but reproducible peak, which corresponded to the d-spacing around 3.4 nm (Supplementary Figure 6a). This spacing matched with the calculated {110} spacing (3.4 nm) of the modelled **SOF-g** network (Supplementary Figure 7), reflecting its periodicity in water. The solid-phase synchrotron SAXS profile afforded a quite sharp signal at 2.0 nm, which matched well with the calculated {211} spacing (Supplementary Figure 6b). Moreover, the solid-phase synchrotron small-angle XRD

profile exhibited three broad peaks around 2.8, 1.4 and 0.83 nm (Supplementary Figure 6c), respectively, which matched with the calculated {111}, {222} and {334} spacings. The structural features of SOF-g are similar to other SOFs assembled in a similar fashion (reference). With the framework structure confirmed, its in vitro cytotoxicity was evaluated using Human cancer (HeLa) cells and the Cell Counting Kit-8 (CCK-8) assay (Supplementary Figure 8). It was found that, after incubating for 24 h with **SOF-a** at 35, 180, 370 and 740 μg/mL, the viability of the HeLa cells maintained at 89.1-97.0%, 96.1-100%, 97.0-100%, and 98.0-100%, respectively, showing the low cytotoxicity of this new self-assembled framework.

Fluorescence study for the inclusion of DNAs by SOFs. All the tetrahedral monomers and the corresponding **SOF-a-g** exhibit strong fluorescence. To investigate the inclusion of DNAs in SOFs, the SOF fluorescence was then recorded with incremental addition of six ss- and dsDNAs (ssDNA-21, ssDNA-23, ssDNA-58, dsDNA-21, dsDNA-23, and dsDNA-58, the numeric suffix represents the number of nucleotides in the sequence) (Figure 2 and Supplementary Table 1 and Supplementary Figure 9). For all the experiments, the concentration of the SOFs was kept unchanged ([**1a-g**] = 5.0 or 2.5 μM). Adding the DNA samples to the solution of the SOFs induced significant quenching (**SOF-a**,**b**,**g**) or enhancement (**SOF-c-f**) of the emission of the SOF (Supplementary Figure 10 and 11). Moreover, at both concentrations of the frameworks, this emission quenching or enhancement exhibited a discernible inflection, which corresponded to saturated DNA loading. In contrast, adding excess of monosodium phosphate induced no significant change of the emission of the frameworks (Supplementary Figure 12). These observations supported that both ss- and dsDNAs were included into the interior of the SOFs through multivalent electrostatic interaction.[41,42] Assuming the concentration of the DNAs at the inflection point to be the saturation inclusion concentration, the weight% of the DNAs included by the SOFs can be calculated (Supplementary Tables 2 and 3). It was found that at [**1**] = 5.0 μM, the SOF carriers could include 18-70w% of ssDNAs and 14-32w% of dsDNAs, whereas at [**1**] = 2.5 μM, the values were 12-43w% and 19-32w%, respectively.

The fluorescence quenching of single- and double end-labeled DNAs (Cy5-ssDNA-21, Cy5-ssDNA-58, Cy5-ssDNA-21-FAM, HEX-ssDNA-21-Cy5, and Cy5-ssDNA-58-FAM) (Supplementary Table 1) by SOFs was also investigated. In all the cases, the quenching of the fluorescence probes also displayed an inflection when about 6~20 molar equivalent of SOFs was added (Figures 2g-l and Supplementary Figures 13-20), and the longer DNA requires more equivalent of SOFs for reaching the saturation. When normalized by the cation/anion charge ratio, the above equivalence translates to a ratio of 1.0~1.4 between the total cation concentration of SOF and the total anion concentration of the DNA. These results strongly support that these DNA strands are effectively included within the frameworks to reach a charge balance.

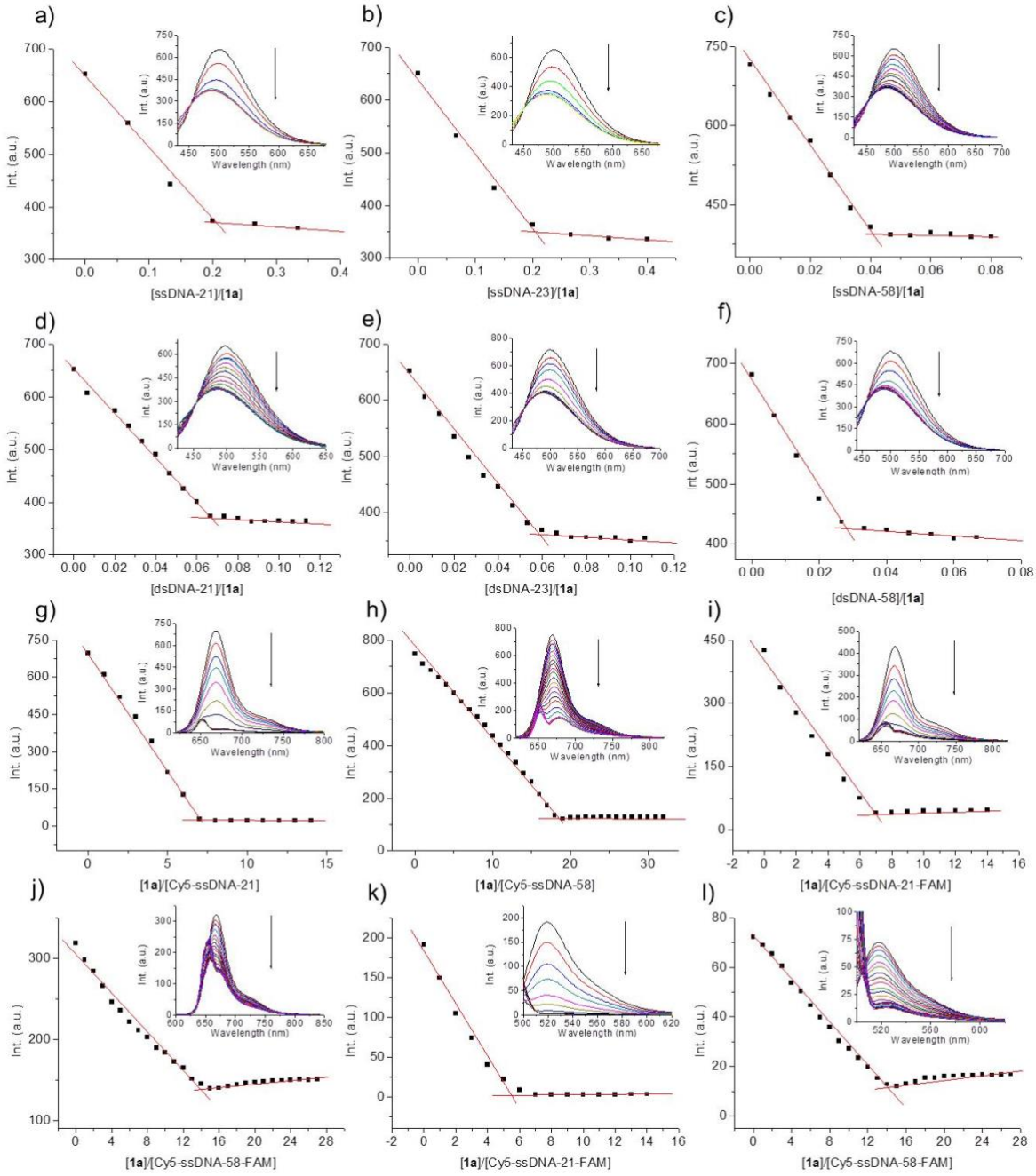

Fig. 2 | Fluorescence titration experiments. Fluorescence quenching plots of **SOF-a** ([**1a**] = 5.0 μM) in water with the addition of (a) ssDNA-21, (b) ssDNA-23, (c) ssDNA-58, (d) dsDNA-21, (e) dsDNA-23, and (f) dsDNA-58. **SOF-a**-induced fluorescence quenching plots of (g) Cy5-ssDNA-21 (λ = 670 nm), (h) Cy5-ssDNA-58 (λ = 670 nm), (i) Cy5-ssDNA-21-FAM (Cy5, λ = 670 nm), (j) Cy5-ssDNA-58-FAM (Cy5, λ = 670 nm), (k) Cy5-ssDNA-21-FAM (FAM, λ = 518 nm), and (l) Cy5-ssDNA-58-FAM (FAM, λ = 518 nm), highlighting a clear inflection point in every titration.

Isothermal titration calorimetric (ITC) experiments. To quantitatively evaluate the inclusion of SOFs for DNAs,[44] ITC experiments were performed for **SOF-a** and **SOF-g** and the above six ss- and dsDNAs (Figure 3 and Supplementary Figures 21a-d). As the inclusion occurred homogeneously, it was expected that, once being included into the interior of the frameworks, linear

nucleic acids might adopt extended or crooked conformations. Control ITC experiments revealed that neither monosodium phosphate nor simple nucleotides interacted with SOFs. Thus, the strong interactions between SOFs and nucleic acids can be attributed to mainly the multivalent electrostatic interactions between the pyridinium or isoquinolinium cations and the phosphate anions of nucleic acids. As a simplified treatment of the complicated binding event, the total cation and anion concentrations of the two respective species were kept at a 1:1 ratio. The titration data was then used to derive apparent binding constants for the ion-pair complexes of ssDNA-21⊂**SOF-a**, ssDNA-23⊂**SOF-a**, dsDNA-21⊂**SOF-a** and dsDNA-21⊂**SOF-a** to be 1.44×10^5, 1.96×10^5, 1.65×10^5 and 9.3×10^4 M^{-1}, respectively. For the four ion-pair complexes of **SOF-g**, the values were determined to be 5.35×10^5, 2.66×10^5, 2.39×10^6, and 5.85×10^6 M^{-1}, respectively. All the results indicated strong binding of SOFs towards the DNAs. Titration experiments were also conducted for longer ssDNA-58, which exhibited more complicated exo- and endothermic phenomena and could not be treated as for the shorter ones (Supplementary Figure 21e). The ITC experiments also revealed that for all the systems studied, the inclusion was driven enthalpically and entropically. The enthalpic contribution should come from the enhanced intermolecular ion-pair interaction. Whereas the entropic contribution could be rationalized by considering that the included DNAs might, to a great extent, cover the hydrophobic surfaces of the SOFs and consequently release the high energy water molecules of low freedom from the hydrophobic surfaces.[45]

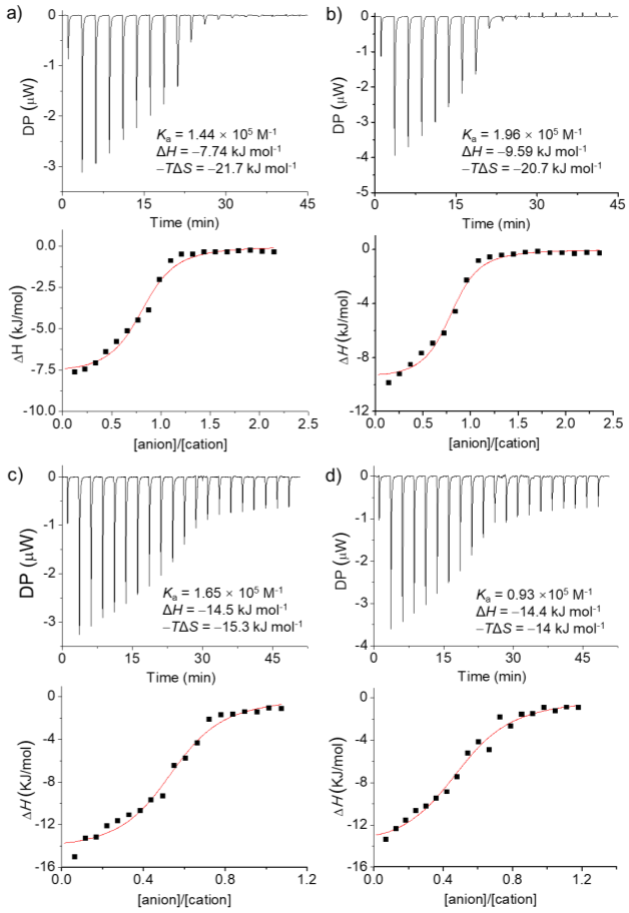

Fig. 3 | ITC experiments. Isothermal titration thermograms of (a) ssDNA-21 ([anion] = 2.1 mM), (b) ssDNA-23 ([anion] = 2.3 mM), (c) dsDNA-21 ([anion] = 0.84 mM), and (d) dsDNA-23 ([anion] = 0.92 mM) into the solution of **SOF-a** ([cation] = 0.20 mM) at 25 °C. The injection volume of the DNAs was 2 μL. [anion] represents the total phosphate concentration of the DNAs and [cation] represents the total pyridinium concentration of **SOF-a**.

Intracellular delivery. Previous studies demonstrated that SOFs could quickly enter cells after incubation and deliver dianionic pemetrexed into tumor cells through endocytosis.[33] The intracellular delivery of SOFs for short DNAs was then investigated using Cy5-labeled ssDNA (Cy5-ssDNA-21) for 293A cell line by staining the nuclei with 4',6-diamidino-2-phenylindole (DAPI) and the cells with adducin α-antibody (H-100, ADD), respectively. After incubation with Cy5-ssDNA-21⊂**SOF-a** (0.25 and 14 μg, respectively) for 4 h, the cells were examined by confocal laser scanning microscopy (CLSM). It was found that the fluorescence signal of the Cy5 dye was very clear and highly overlapped with that of DAPI-stained nuclei and ADD-stained cells. In contrast, in the absence of **SOF-a**, no fluorescence of the Cy5 dye was observed for free Cy5-ssDNA-21 of the identical dosage (Supplementary Figure 22), clearly supporting that **SOF-a** was

capable of delivering Cy5-ssDNA-21 into 293A cells. We then further examined the delivery of more amount of Cy5-ssDNA-21 (2.5 μg) into 293A cells by **SOF-a** and the commercial reagent Lipo2000 at the identical dosage (7.0 μg) in the presence of fetal bovine serum (FBS, 5%). As expected, within the time studied (up to 2 h), no endocytosis of Cy5-ssDNA-21 (2.5 μg) was observed in the absence of added carriers. For cells treated with Lipo2000, weak fluorescence of the Cy5 dye was observed in the cells within 1 h. However, no uniform transfection could be achieved even after 2 h (Figure 4 and Supplementary Figure 23). In contrast, with the treatment of **SOF-a** at the same dosage, the fluorescence of the Cy5 dye was considerably stronger and uniform transfection was observed in 2 h.

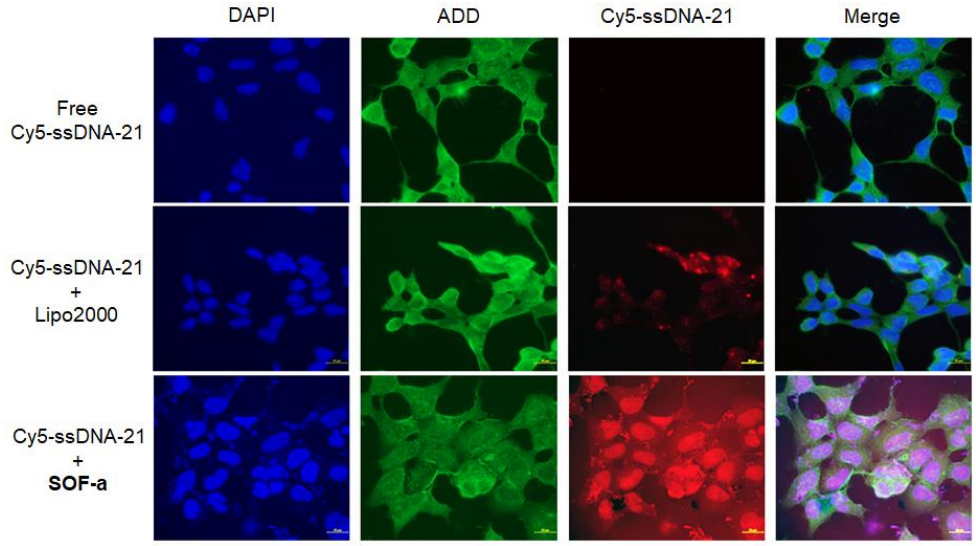

Fig. 4 | Intracellular delivery of Cy5-ssDNA-21 by SOF-a. Confocal laser scanning microscopic images of 293A cells after incubation for 2 h with Cy5-ssDNA-21, Cy5-ssDNA-21⊂Lipo2000 and Cy5-ssDNA-21⊂**SOF-a**. The amount of ssDNA, Lipo2000 and **SOF-a** used was 2.5, 7.0 and 7.0 μg, respectively. Nuclei were stained with DAPI (blue), and cells were stained with ADD (green).

The intracellular delivery of DNAs using SOF carriers was then further tested using flow cytometry. Testing was first conducted with Cy5-ssDNA-21 (2.5 μg) for 293A cell line. Again, Lipo2000 (7.0 μg) was used for comparison and the results were recorded after incubation in 10% FBS for 15 min, 1 h and 2 h to get insight into the delivery process (Figure 5a and supplementary Figure 24). In the absence of a carrier, no intracellular DNA delivery was observed. In 15 min, Lipo2000 and **SOF-a,b,d-g** (7.0 μg) induced 0.1% to 8.9% transfection, suggesting their negligible

or low delivery efficacy, whereas **SOF-c** realized a remarkable 45.2% transfection. In 1 h and 2 h, the transfection efficiency of **SOF-c** reached 93% and 98.9%, which were again significantly higher than that of Lipo2000 (27.2% and 57.5%) and other SOFs, whereas the transfection efficacy of **SOF-a,e-g** was comparable or higher than that of Lipo2000. These tests have also shown very good repeatability (Supplementary Figure 25). Control experiments show that under the identical experimental conditions, tetrahedral monomers **1a-g** exhibited limited transfection efficacy (Supplementary Figure 26) with **1a** and **1c** showing the highest efficacy of 19.1-27.7% and 13.2-17.7%. This result strongly supports that the porous architectures of **SOF-a-g** remarkably enhanced their capacity of including and transfecting nucleic acids.

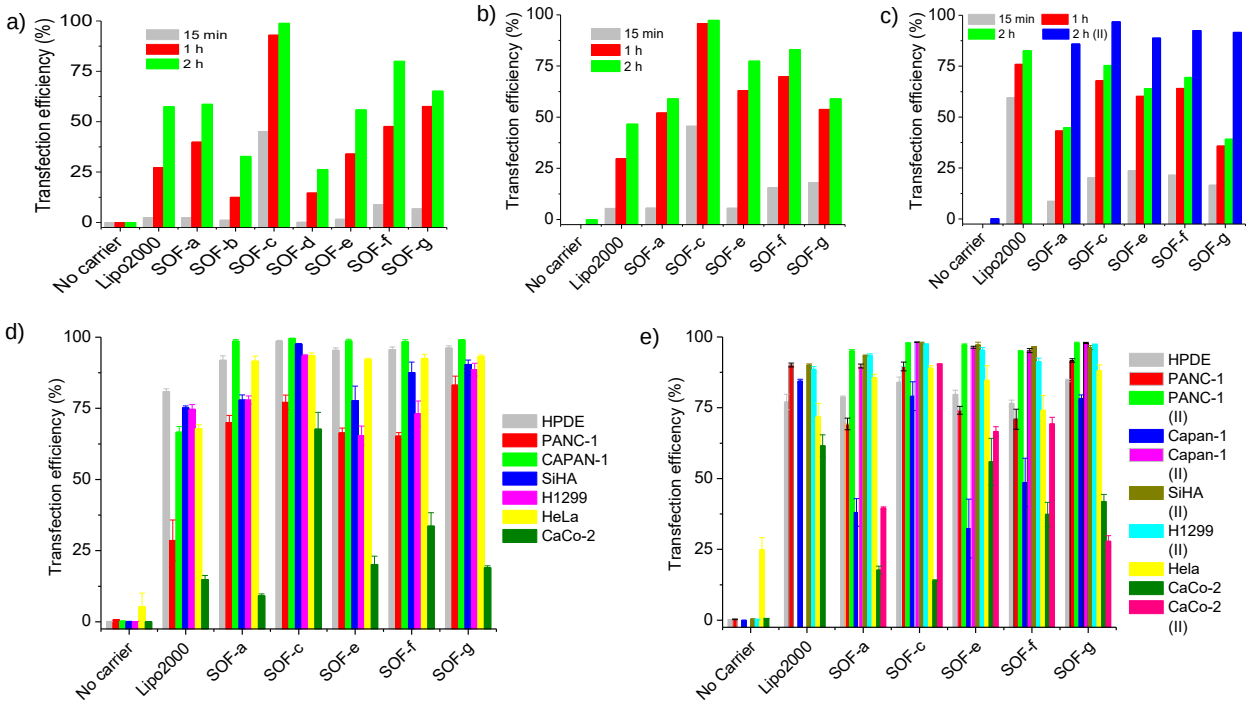

Fig. 5 | Transfection experiment of Cy5-labeled DNAs by SOFs: (a) Cy5-ssDNA-21 (2.5 μg) by **SOF-a-g** (7.0 μg) for 293A cell line, (b) Cy5-dsDNA-21 (4.8 μg) by **SOF-a,c,e-g** (7.0 μg) for 293A cell line, (c) Cy5-dsDNA-58 (4.8 μg) by **SOF-a,c,e-g** (7.0 μg or 56 μg for blue) for 293A cell line, (d) Cy5-ssDNA-21 (2.5 μg) by **SOF-a,c,e-g** (7.0 μg) for HPDE, PANC-1, Capan-1,SiHA, H1299, HeLa, and CaCo-2 cell lines, and (e) Cy5-dsDNA-21 (4.8 μg) by **SOF-a,c,e-g** (7.0 or 14 μg) for HPDE, PANC-1, Capan-1, SiHA, H1299, HeLa, and CaCo-2 cell lines. Lipo2000: 7.0 μg for ssDNA and 14 μg for dsDNA. II: 14 μg of SOFs.

Because **SOF-b** and **SOF-d** generally exhibited the lowest transfection efficacy, we then focused on other SOFs **SOF-a,c,e-g** and extended the investigation to determine their potentials in

transfecting Cy5-ssDNA-21 (2.5 μg) into different cell lines, including HPDE and six cancer cells (PANC-1, Capan-1, SiHA, H1299, Hela and CaCo-2). The detections were all performed after incubation in 10% PBS for 2 h (Figure 5d and Supplementary Figures 27-30). In the blank test without the carriers, about 5% of Hella cells were transfected by passive transportation of the nucleic acid, whereas all other cells underwent less than 1% of transfection. With Lipo2000 (7.0 μg) as the carrier, the transfection efficiency of the seven cell lines was 80.0-81.9%, 20.3-33.0%, 64.5-68.3%, 73.6-76.6%, 70.0-81.9%, 66.4-69.1%, or 13.3-16.1%, respectively. With SOFs (7.0 μg) as the carriers, in all 35 SOF cases, 32 systems displayed transfection efficiency that was higher than that of Lipo2000 for the same cell line, except that of H1299 by **SOF-e** (61.9-68.5%) and **SOF-f** (68-76.3%) and of CaCo-2 by **SOF-a** (8.4-9.6%). Moreover, for all the seven cell lines, the transfection efficacy of **SOF-c** and **SOF-g** was always higher than Lipo2000. In addition, among the 35 series, 19 samples reached >90% of transfection efficiency and 10 samples reached >95% of transfection efficiency.

The intracellular delivery of the above five SOF carriers for Cy5-dsDNA-21 (4.8 μg), which is composed of Cy5-ssDNA-21 and the complementary single-stranded DNA of 21 nt, into 293A cell line was then investigated (Figure 5b and Supplementary Figure 31). Blank test showed that the transfection of the cells by passive diffusion of the nucleic acid was negligible. Preliminary test showed that the transfection efficacy of Lipo2000 was considerably lower and thus its amount was increased to14 μg, whereas that of the SOF carriers was still unchanged (7.0 μg). However, in all cases detected at different times (15 min, 1 h, and 2 h), the five SOF carriers still exhibited higher transfection efficiency than Lipo2000. Remarkably, **SOF-c** could realize 95.7% of transfection efficiency in 1 h, and 97.3% in 2 h. The other four SOFs could induce 59%-83% of transfection efficiency in 2 h, whereas in the same timeframe, Lipo2000 could only reach 46.6%.

The transfections of the five SOFs for HPDE, PANC-1, Capan-1, SiHA, H1299, HeLa, and CaCo-2 cell lines were then further tested (Figure 5e and Supplementary Figures 32-35). For this series of experiments, the amounts of Cy5-dsDNA-21 and Lipo2000 were also maintained at 4.8

and 14 μg, whereas the SOF carriers was tested at two doses of 7.0 and 14 μg. Lipo2000 exhibited 60.6%-90.1% of transfection efficiency. Compared with that of the corresponding cell line, 34 out of the total 50 SOF samples exhibited higher transfection efficacy, with 14 reaching over 90% of transfection efficacy. Among the 25 samples using 14 μg of SOFs, 23 exhibited higher transfection efficiency than that of the Lipo2000 reference.

Finally, we also tested the transfection of the longer Cy5-dsDNA-58 in the 293A cell line, which is composed Cy5-ssDNA-58 and the corresponding un-labeled complementary nucleic acid of 58 nt (Figure 5c and Supplementary Figures 36). At the dose of 4.8, 14 and 7.0 μg for DNA, Lipo2000 and SOFs, respectively, the transfection efficiency of the five SOFs was all lower than that of Lipo2000 after 15 min, 1 h or 2 h of incubation. The Lipo2000-assisted transfection efficacy was. However, when the dose of SOFs was increased to 56 μg, their transfection efficiency in 2 h all surpassed Lipo2000 (82.6%), with **SOF-c** realizing a highest efficiency of 96.8%.

Discussion

The driving forces for the inclusion of DNAs by SOFs were mainly electrostatic attraction and hydrophobicity. Because the inclusion occurred homogeneously, the release of the included DNAs should highly depend on the above two interactions. The dynamic feature of this inclusion process suggests that the included DNA could be released through simple diffusion. Previous in vivo fluorescence imaging of **SOF-a** showed that the framework accumulated in tumor cells and then was metabolized or degraded in cells.[33] Thus, another important route for the release of the included DNA was through the decomposition of the framework. The above CLSM experiments also indicated that the labeled DNAs diffused into all the area of the nuclei, as observed for the delivery of molecular drugs.

In summary, we demonstrate that water-soluble supramolecular organic frameworks can efficiently include short DNAs in a homogeneous manner and realize intracellular delivery into both normal and cancer cells. With the identical carrier loading, in most cases, supramolecular organic frameworks exhibit higher transfection efficacy than the commercial reagent Lipo2000,

with SOF-c exhibiting the most promising transfection efficacy. These water-soluble self-assembled entities represent a novel class of off-the-shelf gene-delivery carriers that feature easy formulation, high stability and in situ DNA inclusion. In the future, this promising strategy will be explored for the transfection of siRNA.

Acknowledgements

We thank National Natural Science Foundation of China (Nos. 21432004 and 21529201) for financial support, Shanghai Synchrotron Radiation Facility for providing BL16B1 and BL14B1 beamlines for collecting the synchrotron X-ray scattering and diffraction data, and the SIBYLS Beamline 12.3.1 of the Advanced Light Source (ALS), Lawrence Berkeley National Laboratory, for collecting solution-phase synchrotron small-angle X-ray scattering data. YL thanks the support from the Molecular Foundry, Lawrence Berkeley National Laboratory, supported by the Office of Science, Office of Basic Energy Sciences, Scientific User Facilities Division, of the U.S. Department of Energy under Contract No. DE-AC02- 05CH11231. The SIBYLS Beamline at ALS was supported through the Integrated Diffraction Analysis Technologies (IDAT) program, supported by DOE Office of Biological and Environmental Research. Additional support comes from the National Institute of Health project MINOS (R01GM105404).

References

1. Anderson, W. French Human gene therapy. *Nature* **392**, 25–30 (1998).
2. Clarke, D. T. W. & McMillan, N. A. J. Gene delivery Cell-specific therapy on target. *Nat. Nanotech.* **9**, 568–569 (2014).
3. Wang, H.-X., Li, M., Lee, C. M., Chakraborty, S., Kim, H.-W., Bao, G. & Leong, K. W. CRISPR/Cas9-based genome editing for disease modeling and therapy: challenges and opportunities for nonviral delivery. *Chem. Rev.* **117**, 9874–9906 (2017).
4. Kuscu, L. & Sezer, A. D. Future prospects for gene delivery systems. *Exp. Opin. Drug Deliv.* **14**, 1205–1215 (2017).
5. Southwell, A. L., Skotte, N. H., Bennett, C. F. & Hayden, M. R. Antisense oligonucleotide therapeutics for inherited neurodegenerative diseases. *Trends Mol. Med.* **18**, 634–643 (2012).
6. Yann, F. & Ferec, C. The potential of oligonucleotides for therapeutic applications. *Trends Biotechnol.* **24**, 563–570 (2006).
7. Ren, K., Liu, Y., Wu, J., Zhang, Y., Zhu, J., Yang, M. & Ju, H. A DNA dual lock-and-key strategy for cell-subtype-specific siRNA delivery. *Nat. Commun.* **7**, 13580 (2016).

8. Shipman, S. L., Nivala, J., Macklis, J. D. & Church, G. M. CRISPR-Cas encoding of a digital movie into the genomes of a population of living bacteria. *Nature* **547**, 345–349 (2017).
9. Robbins, P. D. & Ghivizzani, S. C. Viral vectors for gene therapy. *Pharm. Therap.* **80**, 35–47 (1998).
10. Finer, M. & Glorioso, J. A brief account of viral vectors and their promise for gene therapy. *Gene Therapy* **24**, 1–2 (2017).
11. DiCarlo, J. E., Deeconda, A., DiCarlo, J. E., Deeconda, A., DiCarlo, J. E., Deeconda, A. & Tsang, S. H. Viral vectors, engineered cells and the CRISPR revolution. *Adv. Exp. Med. Biol.* **1016**, 3–27 (2017).
12. Torchilin, V. P. Recent advances with liposomes as pharmaceutical carriers. *Nat. Rev. Drug Discov.* **4**, 145–160 (2015).
13. Buyens, K., De Smedt, S. C., Braeckmans, K., Demeester, J., Peeters, L., van Grunsven, L. A.; de Mollerat du Jeu, X., Sawant, R., Torchilin, V. & Farkasova, K. Liposome based systems for systemic siRNA delivery: Stability in blood sets the requirements for optimal carrier design. *J. Controll. Rel.* **158**, 362–370 (2012).
14. Yang, J., Zhang, Q., Chang, H. & Cheng, Y. Surface-engineered dendrimers in gene delivery. *Chem. Rev.* **115**, 5274–5300 (2015).
15. Paleos, C. M., Tsiourvas, D. & Sideratou, Z. Molecular engineering of dendritic polymers and their application as drug and gene delivery systems. *Mol. Pharmaceutics* **4**, 169–188 (2007).
16. Wang, M., Liu, H., Li, L. & Cheng, Y. A fluorinated dendrimer achieves excellent gene transfection efficacy at extremely low nitrogen to phosphorus ratios. *Nat. Commun.* **5**, 4053 (2014).
17. Pack, D. W., Hoffman, A. S., Pun, S. & Stayton, P. S. Design and development of polymers for gene delivery. *Nat. Rev. Drug Discov.* **4**, 581–593 (2005).
18. Lü, H., Zhang, S., Wang, B., Cui, S. & Yan, J. Toxicity of cationic lipids and cationic polymers in gene delivery. *J. Controll. Rel.* **114**, 100–109 (2006).

19. Son, S., Namgung, R., Kim, J., Singha, K. & Kim, W. J. Bioreducible polymers for gene silencing and delivery. *Acc. Chem. Res.* **45**, 1100–1112 (2012).
20. Hu, J. & Liu, S. Topological effects of macrocyclic polymers: from precise synthesis to biomedical applications. *Sci. China Chem.* **60**, 1153–1161 (2017).
21. Xu, C., Tian, H. & Chen, X. Recent progress in cationic polymeric gene carriers for cancer therapy. *Sci. China Chem.* **60**, 319–328 (2017).
22. Cheng, R., Feng, F., Meng, F., Deng, C., Feijen, J. & Zhong, Z. Glutathione-responsive nano-vehicles as a promising platform for targeted intracellular drug and gene delivery. *J. Controll. Rel.* **152**, 2–12 (2011).
23. Mokhtarzadeh, A., Alibakhshi, A., Yaghoobi, H., Hashemi, M., Hejazi, M. & Ramezani, M. Recent advances on biocompatible and biodegradable nanoparticles as gene carriers. *Exp. Opin. Biol. Therapy* **16**, 771–785 (2016).
24. Nguyen, K. T. & Zhao, Y. Engineered hybrid nanoparticles for on-demand diagnostics and therapeutics. *Acc. Chem. Res.* **48**, 3016–3025 (2015).
25. Feng, L., Zhu, C., Yuan, H., Liu, L., Lv, F. & Wang, S. Conjugated polymer nanoparticles: preparation, properties, functionalization and biological applications. *Chem. Soc. Rev.* **42**, 6620–6633 (2013).
26. Slowing, I. I., Trewyn, B. G., Giri, S. & Lin, V. S.-Y. Mesoporous silica nanoparticles for drug delivery and biosensing applications. *Adv. Funct. Mater.* **17**, 1225–1236 (2017).
27. Zhuang, J., Young, A. P. & Tsung, C.-K. Integration of biomolecules with metal-organic frameworks. *Small* **13**, 1700880 (2017).
28. Peng, S., Bie, B., Sun, Y., Liu, M., Cong, H., Zhou, W., Xia, Y., Tang, H., Deng, H. & Zhou, X. Metal-organic frameworks for precise inclusion of single-stranded DNA and transfection in immune cells. *Nat. Commun.* **9**, 1293 (2018).

29. Tian, J., Zhou, T.-Y., Zhang, S.-C., Aloni, S., Altoe, M. V., Xie, S.-H., Wang, H., Zhang, D.-W., Zhao, X., Liu, Y. & Li, Z.-T. Three-dimensional periodic supramolecular organic framework ion sponge in water and microcrystals. *Nat. Commun.* **5**, 5574 (2014).
30. Tian, Ji., Xu, Z.-Y., Zhang, D.-W., Wang, H., Xie, S.-H., Xu, D.-W., Ren, Y.-H., Wang, H., Liu, Y. & Li, Z.-T. Supramolecular metal-organic frameworks that display high homogeneous and heterogeneous photocatalytic activity for H_2 production. *Nat. Commun.* **7**, 11580 (2016).
31. Tian, J., Chen, L., Zhang, D.-W., Liu, Y. & Li, Z.-T. Supramolecular organic frameworks: engineering periodicity in water through host-guest chemistry. *Chem. Commun.* **52**, 6351–6362 (2016).
32. Tian, J., Wang, H., Zhang, D.-W., Liu, Y. & Li, Z.-T. Supramolecular organic frameworks (SOFs): homogeneous regular 2D and 3D pores in water. *Natl. Sci. Rev.* **4**, 426–436 (2017).
33. Tian, J., Yao, C., Yang, W.-L. Y, Zhang, L., Zhang, D.-W., Wang, H., Zhang, F., Liu, Y. & Li, Z.-T. In situ-prepared homogeneous supramolecular organic framework drug delivery systems (sof-DDSs): Overcoming cancer multidrug resistance and controlled release. *Chin. Chem. Lett.* **28**, 798–806 (2017).
34. Ko, Y. H., Kim, E., Hwang, I. & Kim, K. Supramolecular assemblies built with host-stabilized charge-transfer interactions. *Chem. Commun.* 1305–1315 (2007).
35. Liu, Y., Yang, H., Wang, Z. & Zhang, X. Cucurbit[8]uril-based supramolecular polymers. *Chem. Asian J.* **8**, 1626–1632 (2013).
36. Lagona, J., Mukhopadhyay, P., Chakrabarti, S. & Isaacs, L. The cucurbit[n]uril family. *Angew. Chem. Int. Ed.* **44**, 4844–4870 (2005).
37. Barrow, S. J., Kasera, S., Rowland, M. J., del Barrio, J. & Scherman, O. A. Cucurbituril-based molecular recognition. *Chem. Rev.* **115**, 12320–12406 (2015).
38. Watson, J. D. & Crick, F. H. Molecular structure of nucleic acids; a structure for deoxyribose nucleic acid. *Nature* **171**, 737 (1953).

39. Mandelkern, M., Elias, J. G., Eden, D. & Crothers, D. M. The dimensions of DNA in solution. *J. Mol. Biol.* **152**, 153–161 (1981).

40. Yao, C., Tian, J., Wang, H., Zhang, D.-W., Liu, Y., Zhang, F. & Li, Z.-T. Loading-free supramolecular organic framework drug delivery systems (sof-DDSs) for doxorubicin: normal plasm and multidrug resistant cancer cell-adaptive delivery and release. *Chin. Chem. Lett.* **28**, 893–899 (2017).

41. Hardy, J. G., Kostiainen, M. A., Smith, D. K., Gabrielson, N. P., Pack, D. W. Dendrons with Spermine Surface Groups as Potential Building Blocks for Nonviral Vectors in Gene Therapy. *Bioconjugate Chem.* **17**, 172–178 (2006).

42. Pattni, B. S., Chupin, V. V., Torchilin, V. P. New Developments in Liposomal Drug Delivery. *Chem. Rev.* **115**, 10938−10966 (2015).

43. Wu, Y.-P., Yang, B., Tian, J., Yu, S.-B., Wang, H., Zhang, D.-W., Liu, Y. & Li, Z.-T. Postmodification of a supramolecular organic framework: visible-light-induced recyclable heterogeneous photocatalysis for the reduction of azides to amines. *Chem. Commun.* **53**, 13367–13370 (2017).

44. Privalov, P. L. Microcalorimetry of Macromolecules: The Physical Basis of Biological Structures. *J. Solution Chem.* **44**, 1141–1161 (2015).

45. Silverstein, T. P. The Real Reason Why Oil and Water Don't Mix. *J. Chem. Educ.* **75**, 116–18 (1998).